Grasping visual symmetry

Andrew Blake, Michael Taylor and Adrian Cox
Department of Engineering Science, University of Oxford,
Oxford OX1 3PJ, England

Abstract

Visual representations are chosen to meet the requirements of specified tasks such as object recognition or stereoscopic matching. When vision is regarded as a haptic sense, a new operational description is called for, in support of dextrous manipulation. In the context of two-fingered grasp, an appropriate description can be constructed in terms of local reflectional and rotational symmetry. Related to symmetry-based representations that have been used in pattern and object recognition, its structure is determined, not heuristically, but precisely, by the nature of the grasping task. Its value is demonstrated by its incorporation into the control of a robot that can manipulate objects under visual guidance.

1 Symmetry in images

Reflectional symmetry has been used in image description both in pattern recognition [4] and in vision [7] [15]. The resulting Symmetric Axis Transform (SAT) or local symmetry set captures the underlying structure of "blobs" much as the Voronoi diagram does for point-sets [5].

The suitability of a description is governed by the application. For instance, the codon description for bounding contours [19] is appropriate for the task of sub-part decomposition, as an aid to verbal description of an object. The SAT is appropriate for pattern recognition, reducing shapes to curves which can then be matched. It turns out that a new symmetry-based representation, outlined in this paper, is appropriate when the task is grasping. The representation consists of an ordered set of pairs of points at which an object can be effectively grasped, and which can be defined mathematically, it will be shown, in terms of local symmetry properties. This might be an appropriate representation for a blind agent that learns about objects by feeling them. It might be operative in human preattentive vision, for instance, when a juggler attempts to catch a flaming torch. Such "haptic vision" is an essential supporting mechanism for robot manipulators that operate visually.

2 Symmetry and anti-symmetry sets

The symmetry set of a smooth curve $\mathbf{r}(s)$ has been defined by Bruce and Giblin [8], formalising the mechanism of Blum [4] for shape description . It is the set of centres of bitangent circles to the curve $\mathbf{r}(s)$. This construction is illustrated in figure 1. Alternatively Brady and Asada [7] take the symmetry set as the locus of midpoints of the line joining the bitangent points. A good deal is known about the properties of these sets in relation to the curve. For instance, the set need not be smooth even when the curve is [13]. An alternative geometric representation of the bitangency condition is shown in figure 2a, that the angles between the normals and the line joining the two points on the curve must be equal in magnitude but opposite in sign.

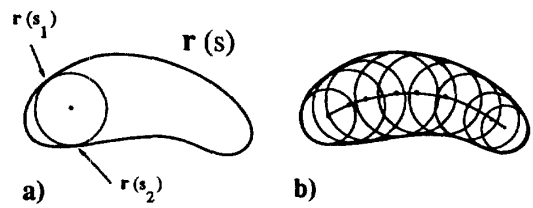

Figure 1: *The symmetry set of a curve* $\mathbf{r}(s)$ *is defined as the locus of centres of bitangent circles.*

The interpretation of the bitangency condition of figure 2a immediately suggests a natural partner to the symmetry set, the anti-symmetry set, in which the angles are equal and of the *same* sign (figure 2b). This is equivalent to choosing pairs of points on the curve with parallel tangents and taking their midpoints. Anti-symmetry has been used previously for capturing global relationships within planar shapes [20]. The anti-symmetry set is also related to the "rotational symmetry set" of Fleck [12] and similarly tends to pick out centres of rotational symmetry. For

0-8186-3870-2/93 $3.00 © 1993 IEEE

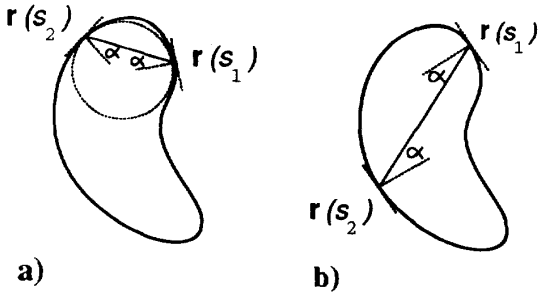

Figure 2: *The symmetry set (a) consists of pairs of curve points which lie on a bitangent circle, or equivalently, for which the angles shown are equal. This suggests immediately also the definition of an antisymmetry set (b).*

instance in the degenerate case of a circle, the anti-symmetry set collapses down to a point at the centre.

Symmetry and anti-symmetry sets can be efficiently computed for object outlines in real images. B-spline approximations to bounding contours are obtained by using a species of closed snake [14] that implodes from the image periphery until it locks onto a feature (figure 3a, 3b). Since the snakes are parameterised as B-splines, the locked snake yields a B-spline representation of the contour. Then anti-symmetry and symmetry sets (figure 3c, 3d) can be computed efficiently [20] and further details are given later in the paper. Whilst the symmetry set for the bell is quite complex, it is apparent that it tends to pick out axes of mirror symmetry between parts of the outline. The anti-symmetry set picks out two-fold rotational symmetries of parts of the outline and contains cusps which indicate dominant centres of symmetry (see the appendix).

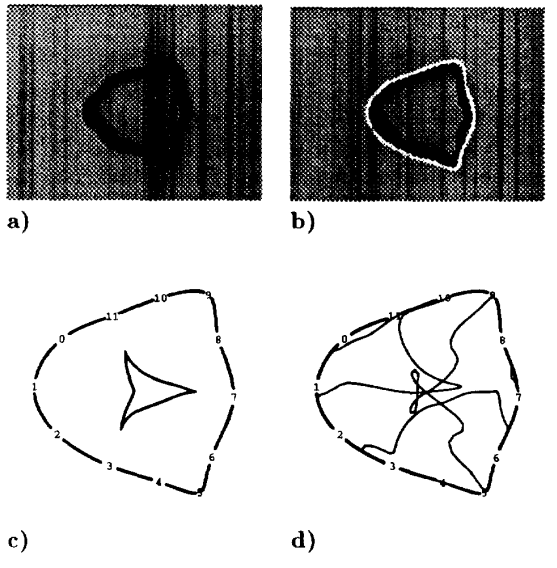

Figure 3: *(a) An image of a bell-shaped cookie-cutter. (b) An imploding, B-spline snake captures the outline of the bell from which both the anti-symmetry set (c) and the symmetry set (d) can be computed.*

3 Properties of the anti-symmetry set

Although the primary purpose of this paper is to relate symmetry to grasp, it is worth digressing briefly to mention two relevant properties of the anti-symmetry set which, unlike the symmetry set, has not been so extensively analysed. The first property is that the anti-symmetry set is an affine invariant, that is, the mapping from a curve to its anti-symmetry set commutes with affine transformation, as in figure 4. Note

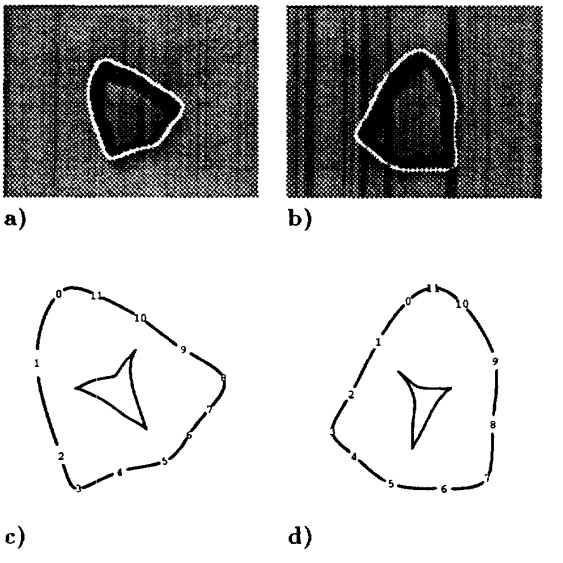

Figure 4: *The bell in figure 3 is imaged here from two new viewpoints (a,b) and since the bell is planar, the outlines in the two views should be related by an affine transformation. The B-spline outlines from the views are shown with their anti-symmetry sets (c,d). Note that the parameterisation, indicated by numbers marked on the curve, is not invariant as it is simply an artifact of the spline fitting process.*

that the symmetry set is *not* an affine invariant. This is illustrated by the case of ellipses which are all re-

lated by affine transformation. For any ellipse, the anti-symmetry set consists of a single point, the centre, and is hence invariant (since the centre of one ellipse transforms affinely to the centre of another). However, the symmetry set of an ellipse consists of its major and minor axes which do *not* generally map to major and minor axes in an affinely transformed ellipse.

The second relevant property is that, generically, the anti-symmetry set contains one or more cusps (an odd number for convex curves) which are affine invariant features of the curve. In principle, this could be useful for model-based vision [17]. Note that the cusps on the anti-symmetry set exist even for convex curves where inflections, for instance, are not available as features on the curve itself. In practice we have not

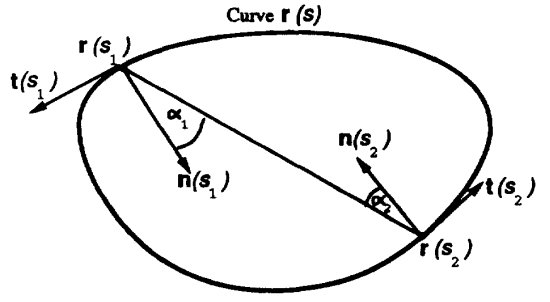

Figure 5: *In a two-fingered grip of a smooth contour* $\mathbf{r}(s)$*, the fingers are placed at* $s = s_1, s_2$*. The line joining the two fingers makes angles* α_1, α_2 *with the normals at* $s = s_1, s_2$ *respectively.*

yet found a contour with fewer than three cusps on its anti-symmetry set and although generically (it can be shown) there may not be two cusps, we have not been able to show that there may not be just one. Three cusps are sufficient to "locate" or "normalise" the curve subject to planar affine transformation. Further details are given in the appendix.

4 Symmetry, anti-symmetry and grasp

The aim of this paper is to establish the relationship between symmetry and two-fingered grasping of planar contours. It turns out that the symmetry and anti-symmetry sets, quite apart from any *descriptive* value they may have for vision, are valuable *operationally* in relating perception to manipulatory action.

4.1 Finger contact

It will be assumed that there are two identical *thin fingers*, small circles in the plane of the object. They are placed on the outline $\mathbf{r}(s)$ at $s = s_1, s_2$ and make a frictional contact with the curve, with coefficient of friction $\mu \geq 0$. The vector joining the fingers makes angles α_1, α_2 with the curve normals, as shown in figure 5. An addition to the thin-fingered gripper, the parallel-jaw gripper is commonly used in practice. Parallel-jaw grasps can be considered as a special case of thin-fingered ones, exactly those grasps that are antisymmetric. The main technical result of this paper,

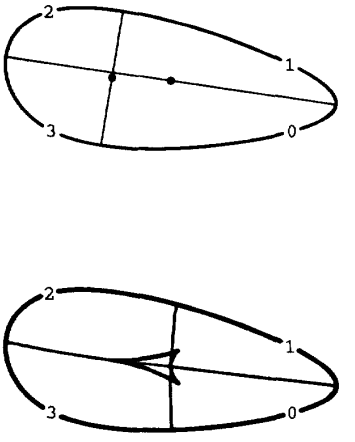

Figure 6: *a) A generic egg with two "type 1" optimal grasps as shown, with midpoints marked. b) The symmetry (thin) and anti-symmetry (thick) sets for the egg, which intersect four times. Two of those four intersections are midpoints of the optimal grasps shown in a).*

to be made precise later, is that any grasp that is optimal in the sense that perturbing the finger positions only increases the friction needed, is either symmetric or anti-symmetric. Of these, the most favourable, type 1, require only infinitesimal friction for equilibrium. They are both symmetric and anti-symmetric. Such grasps are illustrated in figure 6 for a generic egg.

It is clear from the figure that the intersection of the symmetry and anti-symmetry sets can only be a *necessary* condition for type 1 optimal grasps, not a sufficient one; there are four intersections of the sets but only two indicate type 1 grasps. The other two are spurious. Even in the case of the two that are not spurious there is no straightforward mapping from the position of the midpoint of the grasp, at the set intersection, back to the positions of the two fingers them-

selves. Apparently an inconvenient representation of the symmetry sets is being used. For the purpose of characterising grasp, it will prove more effective to represent the sets in *configuration space* (C-space) [11], that is on a diagram whose axes are s_1, s_2, the parametric positions of the two fingers themselves.

4.2 Symmetry and anti-symmetry sets in configuration space

Symmetry and anti-symmetry sets $\mathcal{S}, \mathcal{A}$ can be defined in configuration space as

$$\mathcal{S} = \{(s_1, s_2) : \tan\alpha_1 = -\tan\alpha_2,\ s_1 \neq s_2\} \quad (1)$$

and

$$\mathcal{A} = \{(s_1, s_2), \tan\alpha_1 = \tan\alpha_2,\ s_1 \neq s_2\}. \quad (2)$$

The sets $\mathcal{S}, \mathcal{A}$ are illustrated for the generic egg in figure 7. Note that the sets will always be symmetrical about the $s_1 = s_2$ line since this corresponds simply to exchange of fingers. It is apparent that there are just two intersections of the sets, corresponding to the two type 1 grasps. In the new representation, intersection of the sets is a necessary and sufficient condition for a type 1 grasp. Moreover, for type 1 and for other optimal grasps (type 2 — see later) the locations of the two fingers can be read directly from the C-space diagram, unlike the image-plane representation of the sets which is obscure in this sense.

5 Problem framework and definitions

The main result of the following section is a theorem to the effect that the optimal two-finger grasps of a planar curve lie on the curve's symmetry set or antisymmetry set, or on both. From the point of view of robotics, this gives a relatively general analysis of grasp, free of the need to assume a particular value for the coefficient of friction μ, in contrast with the quantitative analysis of Faverjon and Ponce (1992). First, in this section, the mathematical framework and notation is set up.

5.1 Smooth curve

The bounding curve of the object is a planar vector-valued function $\mathbf{r}(s), s \in \mathcal{I}$ of an arclength parameter s over a set $\mathcal{I}$. It is free of self-intersections and assumed to be bounded, closed, of finite, non-zero length and twice continuously differentiable. The tangent vector is $\mathbf{t}(s) \equiv (t_1, t_2) = \mathrm{d}\mathbf{r}/\mathrm{d}s$, a unit vector. The curve is oriented by the inward unit normal vector $\mathbf{n}(s) = (-t_2, t_1)$, pointing into the object.

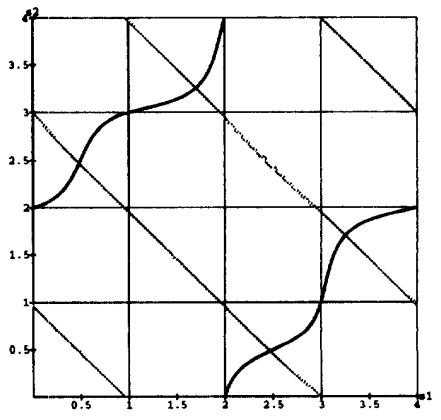

Figure 7: *The symmetry set (grey) and anti-symmetry set (black) for the generic egg of figure 6 are represented here in configuration space. The intersections of the sets correspond to the two type 1 optimal grasps shown in figure 6a.*

5.2 Friction

The friction angles α_1, α_2 can be defined in terms of the tangents and normals shown in figure 5:

$$\cos\alpha_1 = -\mathbf{n}(s_1)\cdot\hat{\mathbf{R}}(s_1, s_2) \quad (3)$$

$$\sin\alpha_1 = \mathbf{t}(s_1)\cdot\hat{\mathbf{R}}(s_1, s_2), \quad (4)$$

and similarly for α_2, where the vector joining the fingers is $\mathbf{R}(s_1, s_2) = (\mathbf{r}(s_1) - \mathbf{r}(s_2))$ and $\hat{\mathbf{R}} = \mathbf{R}/|\mathbf{R}|$.

5.3 Equilibrium

A grasp is in equilibrium when each finger lies within the friction cone of the other [18] [11], as in figure 8. This is equivalent algebraically to satisfying simultaneously the condition

$$|\tan\alpha_1| < \mu \ \text{ and } \ |\tan\alpha_2| < \mu \quad (5)$$

that magnitudes of the friction angles are not too great, and the condition

$$\cos\alpha_1 \cos\alpha_2 > 0 \quad (6)$$

that curve normals at the two fingers are opposed. This covers both the case of compressive grasp when $\cos\alpha_1 > 0,\ \cos\alpha_2 > 0$, and of expansive grasp when $\cos\alpha_1 < 0,\ \cos\alpha_2 < 0$.

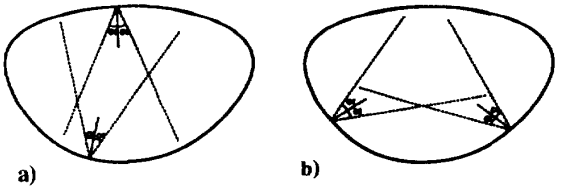

Figure 8: *The two-fingered grip in a) is in equilibruim. The fingers make contact at the two points shown on the contour. Each point lies within the friction cone of the other (semi-angle $\alpha = \tan^{-1}(\mu)$, where μ is the coefficient of friction). In b) there is no equilibrium.*

5.4 Distance function and grasp map

Two mathematical constructs needed to prove the theorem relating grasp and symmetry are the *distance function*

$$R(s_1, s_2) = |\mathbf{R}(s_1, s_2)| \tag{7}$$

which is the length of the vector $\mathbf{R}$ between the contact points of the two fingers, and the *grasp map*

$$G(s_1,s_2) \equiv (G_1(s_1,s_2), G_2(s_1,s_2)) = \left(\frac{\partial R}{\partial s_1}, \frac{\partial R}{\partial s_2}\right) \tag{8}$$

It is straightforward to show that, provided $R \neq 0$,

$$\frac{\partial R}{\partial s_i} = \sin\alpha_i, \quad i = 1, 2. \tag{9}$$

5.5 Friction function

The test (5) above can be expressed in terms of the *friction function*

$$F(s_1, s_2) = \max(|G_1(s_1, s_2)|, |G_2(s_1, s_2)|). \tag{10}$$

The set $\mathcal{E}_\mu$ of force closure grasps, for a given coefficient of friction μ, is then

$$\mathcal{E}_\mu = \{(s_1, s_2) \in \mathcal{I}^2 : s_1 \neq s_2,\ \cos\alpha_1 \cos\alpha_2 > 0,$$

$$F(s_1, s_2) < \sin(\tan^{-1}\mu)\}. \tag{11}$$

Faverjon and Ponce [11] illustrate the set $\mathcal{E}_\mu$ in the C-space (configuration or parameter space) $\mathcal{I}^2$ of the curve. They also show how the boundaries of the set can be efficiently computed for spline curves by expressing the bounding curves

$$\tan\alpha_i = \pm\mu, \quad i = 1, 2$$

in terms of polynomial equations and applying a continuation method to solve them.

5.6 Valid grasp

A grasp is defined to be a configuration $(s_1, s_2) \in \mathcal{I}^2$ such that, for some finite coefficient of friction $\mu \geq 0$, $(s_1, s_2) \in \mathcal{E}_\mu$. In particular, the case $s_1 = s_2$, in which fingers coincide, is excluded. Equivalently, grasps are pairs $(s_1, s_2) \in \mathcal{I}^2$ for which $s_1 \neq s_2$ and $\cos\alpha_1 \cos\alpha_2 > 0$ which is the auxiliary condition (6) for force closure.

6 Extremal grasps

Minima of F are of particular interest because they represent locally optimal grasps — grasps for which any perturbation of finger positions only increases the minimum value of μ required for equilibrium. Given that the function F is not smooth everywhere because of the modulus function $|..|$, the extrema of F must be carefully characterised. A point (s_1, s_2) will be called an extremum of F if, for all ds_1, ds_2, $dF \geq 0$, to first order in ds_1, ds_2. It is clear that, for any $\mathbf{r}(s)$, there must be at least one extremum since F is continuous, defined over a compact set and bounded below ($F \geq 0$).

6.1 Type 1 grasps

The simplest kind of extremum, which will be called *type 1*, is a zero of F and hence a minimum. If also (s_1, s_2) is a grasp (see the definition above) it will be called a *type 1 grasp*. Note from (11) that since $F = 0$ at a type 1 grasp, there is force closure provided $\mu > 0$. That at least one type 1 grasp must exist on a smooth, closed curve was shown by Chen and Burdick [9] who refer to type 1 grasps as "antipodal". Furthermore it can be shown that at least one type 1 grasp is accessible to a parallel jaw gripper [1].

6.2 Type 2 grasps

It is reasonable to ask whether extremal grasps will always be of type 1. It would be convenient if that were so, for then the configurations $\mathcal{E}_\mu$ of force closure grasps for varying coefficient of friction μ would be determined qualitatively by behaviour at the limit $\mu \to 0$ of zero friction. The topology of $\mathcal{E}_\mu$ would not change as μ varied. It is easy to show that this is not the case by constructing counterexamples.

Two examples of locally optimal type 2 grasps are given in figure 9, one antisymmetric grasp and one symmetric one. In each case the grasps are locally but not globally optimal. For instance, the "smile" in figure 9a has a type 1 grasp along the vertical axis of mirror symmetry but this grasp would be inaccessible to a parallel-jaw gripper because of concavity, so the nearby type 2 grasps are viable alternative choices. Note, in each of the examples, that the line joining the fingers is not orthogonal to the curve at either

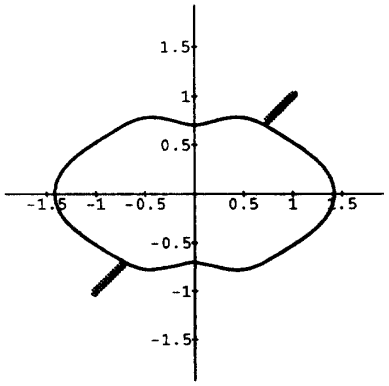

a)

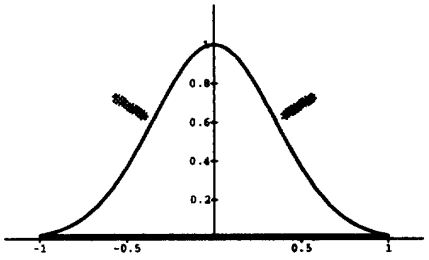

b)

Figure 9: *Type 2 grasps. In both cases shown they are minima representing locally optimal grasps. (a) An antisymmetric grasp on a "smile" curve. It is in equilibrium for $\mu > 0.3$. (b) A symmetric grasp on a "bell" (Gaussian) curve, which is in equilibrium if $\mu > 0.83$.*

finger; this is what makes those grasps type 2 rather than type 1.

6.3 Conditions for optimality

A complete classification of optimal grasps is given by the following theorem.

Theorem 1 (Classification of extrema) *Optimal grasps can be classified as follows:*

Type 1: *intersections of the sets $\mathcal{A}, \mathcal{S}$, which are minima of $F(s_1, s_2)$ with $F(s_1, s_2) = 0$.*

Type 2a: *critical points of G lying on the set $\mathcal{A}$.*

Type 2s: *critical points of G lying on the set $\mathcal{S}$*

A proof of this theorem may be found in the appendix.

The practical consequence of the theorem is that optimal grasps can be located by tracking along the sets $\mathcal{S}, \mathcal{A}$, which are generically smooth, looking for minima of the friction function F restricted to those sets. This is illustrated in figure 10. It is clear from figures 9, 10 and 11 that the extremal grasps, both of type 1 and of type 2, do represent the intuitively natural grasps of an object. A practical grasp planner can select type 1 grasps in descending order of stability. If no type 1 grasp is suitable, for example because of inaccessibility, the type 2 grasps can be examined. It is reasonable to select them in ascending order of the minimum friction required to grasp them.

7 An algorithm for computing robot grasps

We have applied symmetry and anti-symmetry set computation to robot hand-eye coordination in our laboratory. The robot is an ADEPT-1 with a CCD camera built into its end-effector, which has already demonstrated the ability to follow collision-free paths visually [2]. We have added to that the ability to inspect visually an object that is to be picked up and execute a suitable grasp with its gripper (figure 11). We are currently using a parallel-jaw gripper so that all grasps are restricted to the anti-symmetry set $\mathcal{A}$. For this gripper then, it is sufficient to search $\mathcal{A}$ for optimal grasps and we use a fast algorithm to do this, described below.

Since the theory so far applies strictly to planar grasps, three-dimensional grasping as shown in figure 11 must be performed by approximating the extremal contour. The robot executes infinitesimal transverse motion in order to recover the extremal contour from the image motion of the silhouette [6], [3]. Planar regression can be used to check that the extremal contour is approximately planar and to reorient the gripper so that it is orthogonal to the estimated plane. Grasp planning is then applied to the planar approximation of the extremal contour.

7.1 Fast computation of the anti-symmetry set

The anti-symmetry set is produced as an ordered list of C-space points so that the grasp points (type 1 and type 2a) can be found by a simple one dimensional search for minima of α. It can be shown that, in order to achieve adequate smoothness for a stable search for minima, the B-spline used to represent the contour must be of cubic order (or higher). Thus we cannot use the algorithm of Rom and Medioni [20] which applies to quadratic splines, exactly as it stands. Their

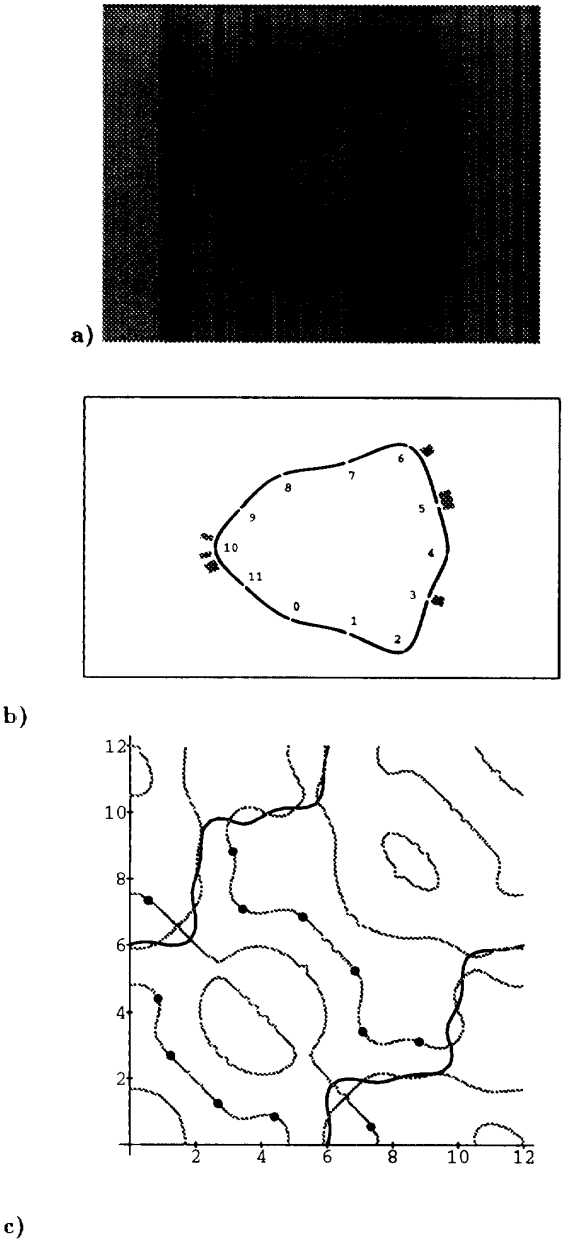

Figure 10: *This bell-shaped cookie-cutter a) has 11 type 1 grasps of which the 3 most stable are displayed in b). The eleven type 1 grasps in c) correspond to the intersections of the antisymmetry set (black) with the symmetry set (grey). The black dots are the type 2 grasps computed by tracking along the symmetry set searching for minima of F.*

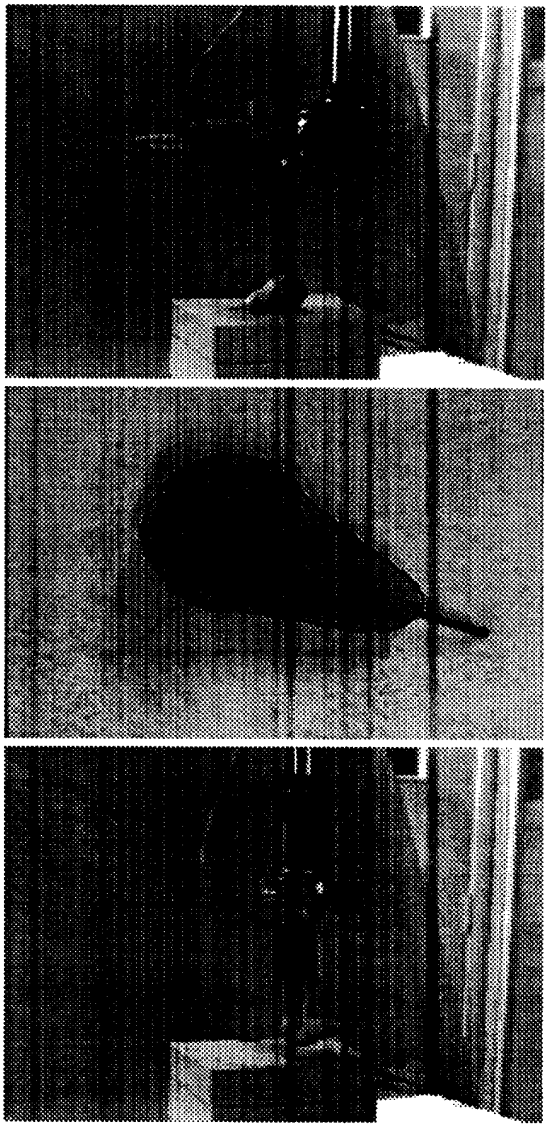

Figure 11: *An ADEPT-1 robot inspects the outline of a fruit visually and plans how to grasp the object with its parallel-jaw gripper.*

algorithm is modified for the cubic case below. Given a cubic B-spline with L spans, and that the spline curve is sampled at N points, the algorithm has an asymptotic time-complexity of $O(N + L^2)$ compared with $O(N^2)$ for the obvious greedy algorithm.

Following Rom and Medioni, the core of the algorithm is a procedure to calculate the anti-symmetry set of a pair of parametric-cubic spans, which can be shown to have the form

$$\alpha(s_1) + \beta(s_1)s_2 + \gamma(s_1)s_2^2 = 0. \qquad (12)$$

where α, β and γ are all quadratic functions of s_1 whose coefficients are derived from the four control points of each span. This means that for a given value of s_1 on one span, the antisymmetric value of s_2 is the solution of the quadratic (12).

The possibility of having two solutions of this quadratic is undesirable, necessitating the tracking of multiple branches of the antisymmetry set simultaneously. If the spans are split into "sub-spans" with constant sign of curvature then, between any pair of sub-spans, (12) has only one solution. This is because, in the absence of inflections, a given tangent on one sub-span is parallel to at most one tangent on the other sub-span. The splitting takes only $O(N)$ time. For a cubic span, there are at most two points of inflection, and hence at most three sub-spans per span so the splitting produces at most $3L$ sub-spans. The anti-symmetry set of a pair of sub-spans is generated in $O(N/L)$ time (N/L is the number of samples on one sub-span). There are $O(L^2)$ pairs of sub-spans in total so overall complexity is $O(NL)$.

Many sub-span pairs have a null anti-symmetry set, as in figure 12 and this can be detected by a fast test. Relying on the fact that sub-spans are free of inflections, it is sufficient to test and compare the gradients at the start and end of each of the two sub-spans. This reduces the asymptotic complexity of the algorithm still further, to $O(L^2 + N)$.

For a thin fingered gripper it is necessary to compute both $\mathcal{A}$ and $\mathcal{S}$ but it is difficult to apply the principles above to compute $\mathcal{S}$ efficiently, though approximations are possible [20]. However, it should be possible, in principle, to compute the symmetry set in $O(NV)$ time, where V is the number of vertices (extrema of curvature [10] on the curve) using the technique of Morris [16] which tracks numerically between singularities of the symmetry set.

8 Conclusions

The important relationship between local symmetry and grasping has been established. Optimal grasps

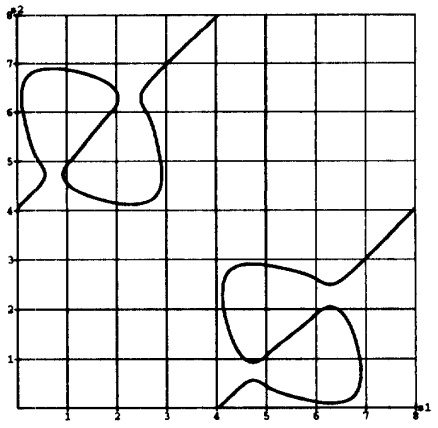

Figure 12: *Computation of the antisymmetry set of a blob, in C-space. Each box is a pairing of sub-spans, to which the basic anti-symmetry set procedure is applied. Empty boxes can be detected by a fast test.*

lie either on the symmetry or antisymmetry sets. Previously, local symmetries have been used as a descriptive tool, a simplifying process for shape descriptors. Consideration of grasping, however, forces an *operational description of shape.* This has the effect both of confirming the descriptive value of local symmetry and modifying it. The most significant modification is to view it in configuration space, rather than in image-space. This has the additional benefit of sidestepping the mathematically fascinating but practically annoying problems of singularity [13] that occur in the image-space representations of the symmetry and anti-symmetry sets.

An outstanding problem is the extension of the theory to three dimensions, continuing to estimate grasps based on a visible silhouette as at present, but to relax the planarity assumption. Structure from motion delivers not a mere space curve (the extremal contour) but a "strip" — a space curve carrying the surface normal. Surface curvature can also be readily computed along such a strip. One possibility would be to seek optimal grasps on that strip, a problem with a 2-dimensional C-space as in the planar case but with more complex geometry. A more ambitious strategy would be to explore viewpoints actively, in search of a silhouette that supports a more stable grasp. Local geometric information from one silhouette would be used to drive the robot to a new vantage point with a

more favourable silhouette.

Acknowledgements

The financial support of the SERC and the EEC is gratefully acknowledged. Discussions with J.M.Brady, A.Zisserman, H.H.Bülthoff, H.C.Longuet-Higgins, P. Winder and P.J.Giblin were most valuable. We thank L.Shapiro and S.Rowe for some careful proof reading.

References

[1] A. Blake. A theory of planar grasp. Technical Report No. OUEL 1958/92, University of Oxford, 1992.

[2] A. Blake, J.M. Brady, R. Cipolla, Z. Xie, and A. Zisserman. Visual navigation around curved obstacles. In *Proc. IEEE Int. Conf. Robotics and Automation*, volume 3, pages 2490–2499, 1991.

[3] A. Blake and R. Cipolla. Robust estimation of surface curvature from deformation of apparent contours. In O. Faugeras, editor, *Proc. 1st European Conference on Computer Vision*, pages 465–474. Springer–Verlag, 1990.

[4] H. Blum. Biological shape and visual science. *Int. J. Theoretical Biol.*, 38:205–287, 1973.

[5] J.D. Boissonat. Representing solids with the delaunay triangulation. In *Proc. ICPR*, pages 745–748, 1984.

[6] R.C. Bolles, H.H. Baker, and D.H. Marimont. Epipolar-plane image analysis: An approach to determining structure. *International Journal of Computer Vision*, vol.1:7–55, 1987.

[7] J.M. Brady and H. Asada. Smooth Local Symmetries and their Implementation. *Int. Journal of Robotics Research*, 3(3), 1984.

[8] J.W. Bruce and P.J. Giblin. *Curves and Singularities*. Cambridge, 1984.

[9] I-M. Chen and J.W. Burdick. Finding antipodal point grasps on irregularly shaped objects. In *IEEE Proc. Robotics and Automation*, pages 228–283, 1992.

[10] M.P. DoCarmo. *Differential Geometry of Curves and Surfaces*. Prentice-Hall, 1976.

[11] B. Faverjon and J. Ponce. On computing two-finger force-closure grasps of curved 2D objects. In *Proc. IEEE Int. Conf. Robotics and Automation*, volume 3, pages 424–429, 1991.

[12] M. Fleck. Local rotational symmetries. In *IEEE Proc. CVPR*, pages 332–337, 1986.

[13] P.J. Giblin and S.A. Brassett. Local symmetry of plane curves. *American Mathematical Monthly*, 92(10):689–707, 1985.

[14] M. Kass, A. Witkin, and D. Terzopoulos. Snakes: Active contour models. In *Proc. 1st Int. Conf. on Computer Vision*, pages 259–268, 1987.

[15] M. Leyton. A process grammar for shape. *J. Artificial Intelligence*, 34:213–247, 1991.

[16] R.J. Morris. *Symmetry of curves and the geometry of surfaces: two explorations with the aid of computer graphics*. PhD thesis, University of Liverpool, 1990.

[17] J.L. Mundy and A.P. Zisserman. *Geometric invariance in computer vision*. MIT Press, 1992.

[18] V.D. Nguyen. Constructing force-closure grasps. *Int. Journal of Robotics Research*, 7(3):3–16, 1988.

[19] W. Richards and D.D. Hoffman. Codon constraints on closed 2D shapes. *CVGIP*, 31:265–281, 1985.

[20] H. Rom and G. Medioni. Hierarchical decomposition and axial representation of shape. *IEEE Trans. Pattern Analysis and Machine Intell.*, in press, 1992.

A Proof of the classification of extrema

The proof of theorem 1 is given here. Recall that the definition of an extremal grasp implies that the case $s_1 = s_2$ (coincidence of fingers) is excluded and hence also $R > 0$. Given the $|..|$ functions in the definition (10) of F, its extrema must be considered as three distinct cases:

1. $G_1(s_1, s_2) = G_2(s_1, s_2) = 0$
2. $|G_1(s_1, s_2)| = |G_2(s_1, s_2)| \neq 0$
3. $|G_1(s_1, s_2)| \neq |G_2(s_1, s_2)|$.

The first two of these three cases are the type 1 and type 2 grasps defined above. The third case never arises and is eliminated as follows. Suppose, without loss of generality, that at such an extremum $|G_1(s_1, s_2)| > |G_2(s_1, s_2)|$ and that $G_1(s_1, s_2) > 0$ then, in a neighbourhood, $F(s_1, s_2) = G_1(s_1, s_2)$ so that, for extremality, we require

$$\frac{\partial G_1}{\partial s_1} = \frac{\partial G_1}{\partial s_2} = 0.$$

Now it can be shown that the second of these equalities implies that $\cos\alpha_1 \cos\alpha_2 = 0$, in violation of the condition (6) for a valid grasp.

Type 1

From (8) and (9), case 1 above arises when $\sin\alpha_1 = \sin\alpha_2 = 0$ which, given (6), is equivalent to satisfying simultaneously the conditions for membership of $\mathcal{S}$ and $\mathcal{A}$ respectively. Such grasps are therefore in $\mathcal{S} \cap \mathcal{A}$ as required. Moreover, from (10), they are zeros of F and hence minima of F — type 1 grasps.

Type 2

Case 2 above arises in one of two ways. Either $G_1(s_1, s_2) = G_2(s_1, s_2)$ so that, from (6), (8) and (9), $\alpha_1 = \alpha_2 = \alpha$ and therefore $(s_1, s_2) \in \mathcal{A}$, or $G_1(s_1, s_2) = -G_2(s_1, s_2)$ with $\alpha_1 = -\alpha_2 = \alpha$ and $(s_1, s_2) \in \mathcal{S}$. These will give type 2a and 2s grasps respectively.

At a type 2 extremum of F, $G_1 = G_2$ and since $F = \max(|G_1|, |G_2|)$ the condition for extremality, for type 2a, is that

$$\mathrm{d}G_1 \mathrm{d}G_2 \leq 0 \text{ for all } \mathrm{d}s_1, \mathrm{d}s_2, \text{ to first order.}$$

(The condition ensures that there exists no step $(\mathrm{d}s_1, \mathrm{d}s_2)$ in C-space for which $|G_1|$ and $|G_2|$ simultaneously decrease.) Now Now

$$\begin{pmatrix} \mathrm{d}G_1 \\ \mathrm{d}G_2 \end{pmatrix} = J \begin{pmatrix} \mathrm{d}s_1 \\ \mathrm{d}s_2 \end{pmatrix},$$

where J is the Jacobian matrix of G, so extremality is achieved when $\det J = 0$ and also

$$J_{11}J_{12} + J_{21}J_{22} \leq 0. \tag{13}$$

Type 2s The condition for extremality, for type 2s, is that

$$\mathrm{d}G_1 \mathrm{d}G_2 \geq 0 \text{ for all } \mathrm{d}s_1, \mathrm{d}s_2, \text{ to first order.}$$

and, using the same reasoning as in the type 2a case, extrema arise on the set $\mathcal{S}$ where $\det J = 0$ □

B Derivation of some properties of the anti-symmetry set

As mentioned earlier in the text, the cusps in the anti-symmetry set indicate dominant centres of two-fold rotational symmetry. Here we show that they arise when the curvatures of the two points on the curve are equal. These special points clearly possess a greater degree of local rotational symmetry than those with equal tangents alone.

For the purpose of the following brief analysis, the anti-symmetry set can be defined in C-space as pairs of parameter values such that:

$$\mathcal{A} = \{(s_1, s_2) : a(s_1, s_2) = 0, s_1 \neq s_2\}$$

where a is defined in terms of the unit tangent vectors at s_1 and s_2 as the function:

$$a(s_1, s_2) = \hat{\mathbf{n}}(s_1) \cdot \hat{\mathbf{t}}(s_2).$$

Differentiating this along $\mathcal{A}$ with respect to s_1 and s_2 it can be shown that:

$$\frac{\partial a}{\partial s_1} = \kappa(s_1)$$

$$\frac{\partial a}{\partial s_2} = -\kappa(s_2).$$

An incremental step along the set $\mathcal{A}$ in C-space of $(\delta s_1, \delta s_2)$ will not change $a(s_1, s_2)$ from zero, and so:

$$\frac{\partial a}{\partial s_2}\delta s_2 + \frac{\partial a}{\partial s_1}\delta s_1 = 0$$

$$\frac{\partial a}{\partial s_2}\frac{\partial s_2}{\partial s_1} = -\frac{\partial a}{\partial s_1}$$

$$\frac{ds_2}{ds_1} = \frac{\kappa(s_1)}{\kappa(s_2)}.$$

This shows that the general (non-unit) tangent to the C-space curve is given by:

$$\mathbf{t}_c = \begin{bmatrix} \kappa(s_2) \\ \kappa(s_1) \end{bmatrix}.$$

The mapping I that transforms the pairs of parameter values in $\mathcal{A}$ from C-space on to the image plane as the locus of mid-points is:

$$I : \Re^2 \mapsto \Re^2, \quad I(s_1, s_2) = \frac{1}{2}\left(\mathbf{r}(s_1) + \mathbf{r}(s_2)\right).$$

The Jacobian of I on $\mathcal{A}$ can be derived as:

$$J_{\mathcal{A}} = \frac{1}{2}\left[(1 - \frac{\kappa(s_1)}{\kappa(s_2)})\hat{\mathbf{t}}(s_1) \quad (1 - \frac{\kappa(s_2)}{\kappa(s_1)})\hat{\mathbf{t}}(s_2)\right].$$

Hence, the local image of the general tangent vector to the C-space curve can now be calculated:

$$\mathbf{t}_i = J_{\mathcal{A}}\mathbf{t}_c$$

$$\mathbf{t}_i = \frac{1}{2}\left[(1 - \frac{\kappa(s_1)}{\kappa(s_2)})\hat{\mathbf{t}}(s_1) \quad (1 - \frac{\kappa(s_2)}{\kappa(s_1)})\hat{\mathbf{t}}(s_2)\right]\begin{bmatrix} \kappa(s_2) \\ \kappa(s_1) \end{bmatrix}$$

$$\mathbf{t}_i = (\kappa(s_2) - \kappa(s_1))\,\hat{\mathbf{t}}(s_1).$$

This shows that the magnitude of the tangent vector in the image plane diminishes to zero as the curvatures of the two points converge, thus forming cusps at points of distinguished local rotational symmetry. It also shows that the tangent to the anti-symmetry set in the image is always parallel to the tangents at the curve. This result helps when interpreting the various figures earlier in the paper.